AN IN SITU INVESTIGATION OF VOID GENERATION AND TRANSPORT DURING RESIN TRANSFER MOULDING BY MEANS OF SYNCHROTRON X-RAY LAMINOGRAPHY

J. Castro[1, 3], L. Helfen[2,4], C. González[1, 3], F. Sket[1]

[1]IMDEA Materials Institute, C/Eric Kandel, 2, 28906 Getafe, Madrid, Spain
Email: jaime.castro@imdea.org, Web Page: http://www.imdea.org
[2]Karlsruhe Institute of Technology, P.O. Box 3640, D-76021 Karlsruhe, Germany
[3]Departmento de Ciencia de Materiales, Universidad Politécnica de Madrid, 28040 Madrid, Spain
[4]European Synchrotron Radiation Facility, ESRF, 71 Avenue des Martyrs, 38000 Grenoble, France

Keywords: Textile composites, Defects, Porosity/voids, Resin Transfer Molding (RTM), Synchrotron-radiation Computed Tomography (SRCL)

Abstract
In this work, Resin Transfer Molding (RTM) experiments were carried out using Synchrotron X-ray Computed Laminography (SXCL) techniques at the European Synchrotron Radiation Facility (ESRF) to study the mechanism of microfluid within a dry fiber preform. A viscous epoxy resin was injected into E-glass at constant flow velocity using an in-house developed device. SXCL images allow the detailed reconstruction of fiber bundles while the contrast between the different phases (air, fluid and fibers) was enough to track the fluid front position and shape as well as the void transport during infiltration. The experimental set up allowed us to analyze the flow along the whole thickness of the part at different process times: prior to void generation, void generation and void transport. The mechanism of void transport was related to the geometry of the layer and the experiment conditions.

1. Introduction

In the RTM process, the dry fiber preform is placed in a mold cavity with the shape of the designed part. The mold is then closed and a liquid plastic resin is injected through one or more inlets by a pressure gradient provided by the application of vacuum dragging the resin and/or the application of a pressure to the resin. The liquid resin penetrates the preform and fills the empty spaces between fiber tows and the space between filaments within the fiber tows impregnating the fibers. Once the filling process is finished, the composite material is cured by the application of a temperature cycle. The resin turns into solid and the part is extracted from the cavity mold. The most limiting drawback in liquid molding is the formation of voids during infiltration and the difficulty to remove them before the curing process ends. The void formation is a consequence of the heterogeneous architecture of the fabric and its placement in the mold which leads to a heterogeneous resin flow inside the fabric. In the fiber bundles, the flow is mainly driven by capillary forces while in the space between bundles the viscous forces, driven by the resin pressure gradient, dominate the flow. This dual-scale flow is the major cause of void formation in liquid molding due to the competition between capillary and viscous forces [1].

Previous experimental observations have demonstrated that void formation depends on the ratio between viscous and capillary forces through the non-dimensional modified capillary number (Ca^*) [2]:

$$Ca^* = \frac{\mu \cdot v}{\gamma \cdot \cos(\theta)} \quad (1)$$

where μ and v stand, respectively, for the resin viscosity and the average resin velocity, while γ and θ are the fluid surface tension and the contact angle between resin and fiber, respectively. In this paper, we will refer to the modified capillary number as the capillary number for simplicity. For high capillary numbers ($Ca^* > 10^{-2}$), viscous forces are prominent so the fluid flows faster between the bundles, generating porosity inside the fiber tows. On the other hand, for low capillary numbers ($Ca^* < 10^{-3}$) the capillary forces are dominant and the velocity within the bundles is much higher. Hence, voids are generated in the spaces between the fiber tows. When capillary and viscous flows are balanced, the capillary number is placed in an optimal range of values that minimize the porosity content. According to [2] the optimal range lies between $10^{-3} < Ca^* < 10^{-2}$.

However, avoiding void generation seems to be an impossible task. For this reason, authors have focused on the void transport mechanisms. Lundström et al. [3] investigated the validity of the theory that establishes the relationship between the required pressure to transport a bubble in a constricted capillary tube with the capillary radius and the surface tension of the liquid. They concluded that it is easier to remove bubbles situated between bundles than voids constricted within the fiber tows. This work was used by Matsuzaki et al. [4] to develop an *in situ* method for measuring void content with an optical microscope. Their results indicate that, close to the inlet, void content (total porosity) decreases as the distance to the inlet increases. However, the injection experiments were not performed at constant velocity. Thus, it is difficult to distinguish between the impact of the resin velocity along the injection direction and the pore mobility on the final void content. In addition, their set up of microscope and video camera did not allow them to analyze the sample through the thickness or the microporosity within the bundles.

Researchers have typically used surface images and videos to analyze the porosity evolution during infiltration in composites. These techniques provide only two-dimensional information of the surface ignoring the information inside the part. Imaging sample interiors in liquid molding is thus essential to understand the mechanisms of void generation and transport within the part and X-Ray Computed Tomography (XCT) emerges as a good candidate for such purposes. X-Ray Computed Tomography (XCT) is a non-destructive technique that provides a three-dimensional volume image represented as a series of 2D slices. For instance, Sisodia et al. [5] analyzed by X-ray tomography the porosity of multiaxial fabric reinforced composites manufactured by RTM process after curing. They concluded that voids are much more unlikely to be situated in the layers where the fibers are parallel to the flow direction. However, the information of the porosity after the whole cure process obtained from *ex situ* tomography, combining the mechanisms of generation and transport and gives no information about how the fluid moves in the specimen. On the other hand, an *in situ* set up can provide information about the fluid motion and would allow studying the mechanisms of void generation and transport. For instance, Vilà et al. [6] carried out *in situ* SXCT (Synchrotron X-ray Computed Tomography) measurements of voids and fluid propagation within a tow of fibers during a step by step infusion process. Due to the large measurement acquisition time, the experiments were observed under quasi-static conditions. They presented the behavior of a non-wetting fluid within a bundle of fibers and the transport of pores through convergent fibers. Continuous infiltration can yield more realistic results. For this reason, Larson et al. [7] also presented *in situ* images of impregnated unidirectional fiber beds during continuous resin infiltration. Contrarily to Vilà's work, the fibers were allocated in a cylindrical rigid mold and controlled pressures were applied in the inlet and in the outlet. Therefore the velocity during the experiments was not constant. They developed a method to predict the permeability in non-uniform fiber beds. In these two works, the infiltration measurements were only observed in fiber bundles, not in a plain woven fabric which is more representative of a composite part.

For this work, we have infiltrated an epoxy resin at constant velocity into a set of E glass layers using a rectangular mold. Contrarily to constant pressure injection, the effect of the velocity on the porosity does not change during the same experiment. Additionally, the injection experiment was performed in a plain

woven fabric structure allowing to study the difference between the capillary and viscous flows. To this end, infiltration of E-glass fibers in a RTM mold was studied *in situ*, for the first time, during Synchrotron-radiation Computed Laminography (SRCL) measurements. This inspection technique is particularly suitable for laminate-shaped samples (large aspect ratio of length and width with respect to the thickness), such as the shape of the plain woven fabric structures. In the laminography configuration, X-rays can avoid thicker directions of the mold since they are not irradiated perpendicular to the sample rotation direction, but at an inclined angle from that direction. Thus, laminography allows for the inspection of specimens maintaining engineering-relevant boundary conditions to observe the flow as closely as possible to a real infiltration process.

2. Experimental techniques

The injection mold was designed specifically to be inspected by SRCL. Thus, the fluid must be infiltrated parallel to the rotation stage. The rigid mold allows containing the dry fiber preform in a cavity of 74mm x 80mm x 1mm (Figure 1.a). The matched mold was made of PMMA so the propagation of the fluid inside can be observed with the naked eye (Figure 1.b). An additional advantage of PMMA is that it has a low X-ray absorption coefficient allowing sufficient X-ray transmission. Two silicone seals were placed between the two the parts of the mold to avoid fluid leaks during the experiment. An in-house syringe pump was manufactured to control the flow during the experiment and it was connected to the inlet of the mold, while atmospheric pressure acted on the outlet.

The sample used for this experiment was a set of six plies of an E-glass plain woven fabric. The average fiber diameter is 16 ± 2 µm. The six layers fit within the mold cavity and were not impregnated with the fluid before the experiment.

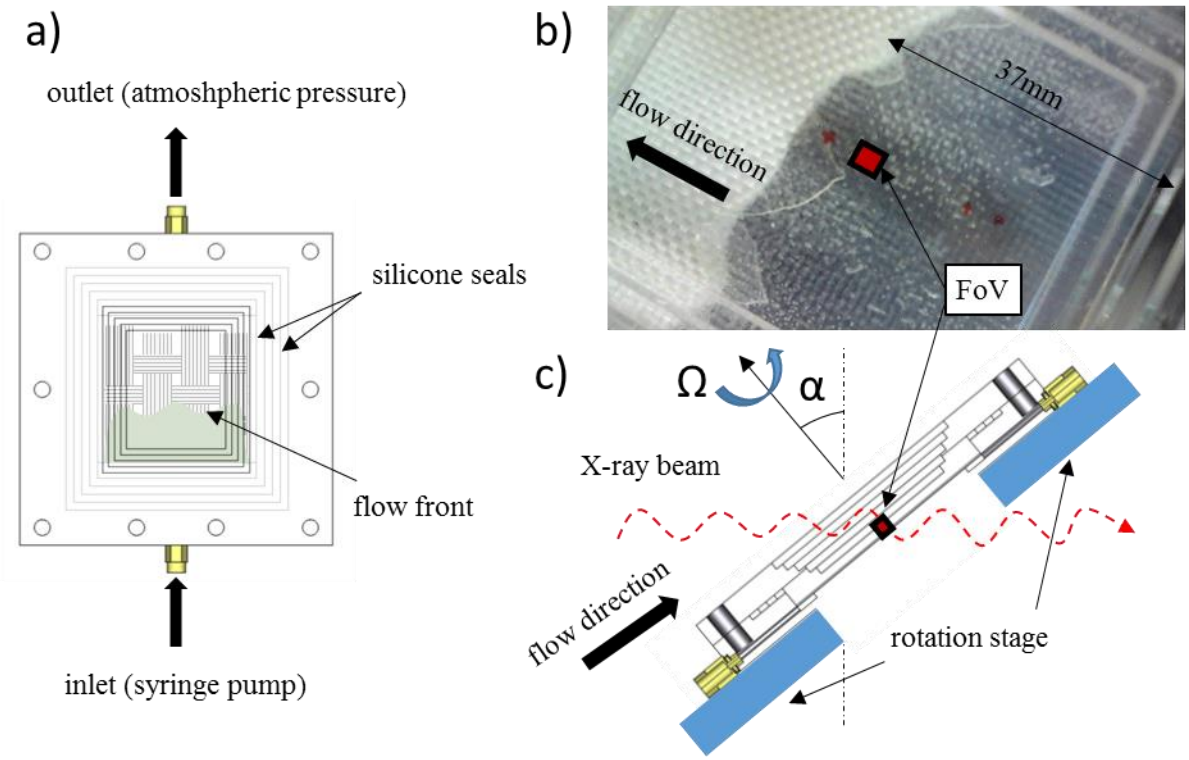

Figure 1. a) Sketch of the device for resin injection in the SCRL beamline. b) Picture of the impregnated fibers during an injection experiment. c) Sketch of the rotating system in the laminography set-up.

A high viscous epoxy resin, D.E.R. ™ 332, was used as infiltration fluid. A 10wt% of a contrast agent (4-Bromophenol) was added to increase the resin absorption coefficient to be able to clearly distinguish the three elements in the tomographic reconstruction: fibers, resin and air. The blend was degassed immediately before the infiltration for 10 min in a vacuum container.

The fluid properties were determined prior to the *in situ* infiltration experiments. The viscosity of the fluid, 1.69 Pa·s, was measured with a rotational viscometer. The surface tension was measured using an adapted version of the classical Wilhelmy Plate method, i.e. using a porous paper instead of a platinum plate. The value obtained was 56 mN/m. The contact angle between resin and E glass fiber was determined from S-XCT observations of a resin infiltrated capillary of the same fiber types. A full statistical analysis of the contact angle was performed leading to a value of 50°. With these properties, the non-dimensional modified capillary number can be calculated with the average linear velocity of the resin. The resin infiltration was performed with two different injection velocities in order to observe different fluid behavior. The resin velocity was calculated from the flow front position at different times during the experiment. The flow front position was measured from a sequence of images taken by a video camera situated above the mold. The calculated velocities and their corresponding capillary number are shown in Table 1.

Table 1. Properties of the fluid and experiment conditions

Experiment	μ (Pa · s)	γ (mN / m)	θ (°)	v (mm/min)	Ca^* (-)
A	1.69	56	50	1.89	$1.4 \cdot 10^{-3}$
B				0.39	$3.0 \cdot 10^{-4}$

The *in situ* experiments were performed at the ID19 microtromography beamline at the ESRF. The synchrotron beam was generated by an undulator PPU13A which produces X-rays with an energy of 26KeV filtered with 5.6 mm aluminum plates. The light emitted by a GGG scintillator was magnified 3 times and collected by a PCO.Edge 5.5 camera, obtaining a resolution of 2.2 µm/pixel and a field of view (FoV) of 5632 x 4752µm^2. Each acquired tomogram consisted of 1799 radiographies plus darks and flats images for further correction of detector imperfections, with an exposure time of 50 ms for each radiography resulting a scan time of 1.8 min per volume. The sample to the detector distance was set to 295 mm and the lamino angle to 32.5° (α in Figure 1.c). For each experiment, several laminography inspections were carried out at positions of the laminates, as well as at different times for each position to allow studying the evolution of resin and voids within the fabric.

3. Results and discussion

The plain woven architecture consists of fiber tows or yarns in two perpendicular directions, called weft and warp. The warp yarns are the longitudinal ones and parallel to the fluid in this study, while the weft yarns are drawn through and inserted over-and-under the warp (weft are perpendicular to the warp yarns and therefore perpendicular to the fluid direction). The gap between the yarns are called resin channels. According to the capillary number calculated for the experiment A (Table 1.), the injection was carried out under optimal Ca^* conditions. This condition indicates that the fluid flows at approximately the same velocity between the bundles and within the bundles. This is visible in Figure 2.a, which shows that the flow front for capillary flow is close to the flow front for viscous flow in the injection direction. Under these conditions, the macroporosity was the minimum found among several experiments. In experiment B, however, the resin flowed faster within the tows than along the channels, which is in accordance with a lower capillary number for this experiment (see Table 1). Figure 2.b elucidates the fluid behavior at low injection velocities. The resin pressure along the channels is not high enough to take up the air situated between the fiber yarns. However, the adhesive forces, i.e. capillary forces, between fiber filaments and resin can drive the flow into the fiber tows. As a result, a clear lead-lag or

fingering can be seen in the flow front with flow leading inside the fiber tows. The length of these fingerings will be determined by the local fabric geometry. When a fingering is generated, the surface tension of the liquid prompts to reduce the liquid surface, pulling the flow between yarns (Figure 2.b). Whereas, the capillary forces pushes forward the resin within the bundles, generating more distance between the local flow fronts in the yarns and in the channels. If adjacent plies do not show nesting (in-phase plies) as in (Figure 2.d), the capillary forces are stronger since the resin can stand on more filament walls to flow forward. For this reason, the fingering length is larger in non-nested plies rather than nested ones. When the fingering within the fiber tows, driven by transversal capillary forces, collapse into one another, they trap the air behind generating a bubble (Figure 2.c). For this reason, the longer the fingerings are, the larger the void is generated. As expected, injections with low capillary numbers generated macroporosity in the channels.

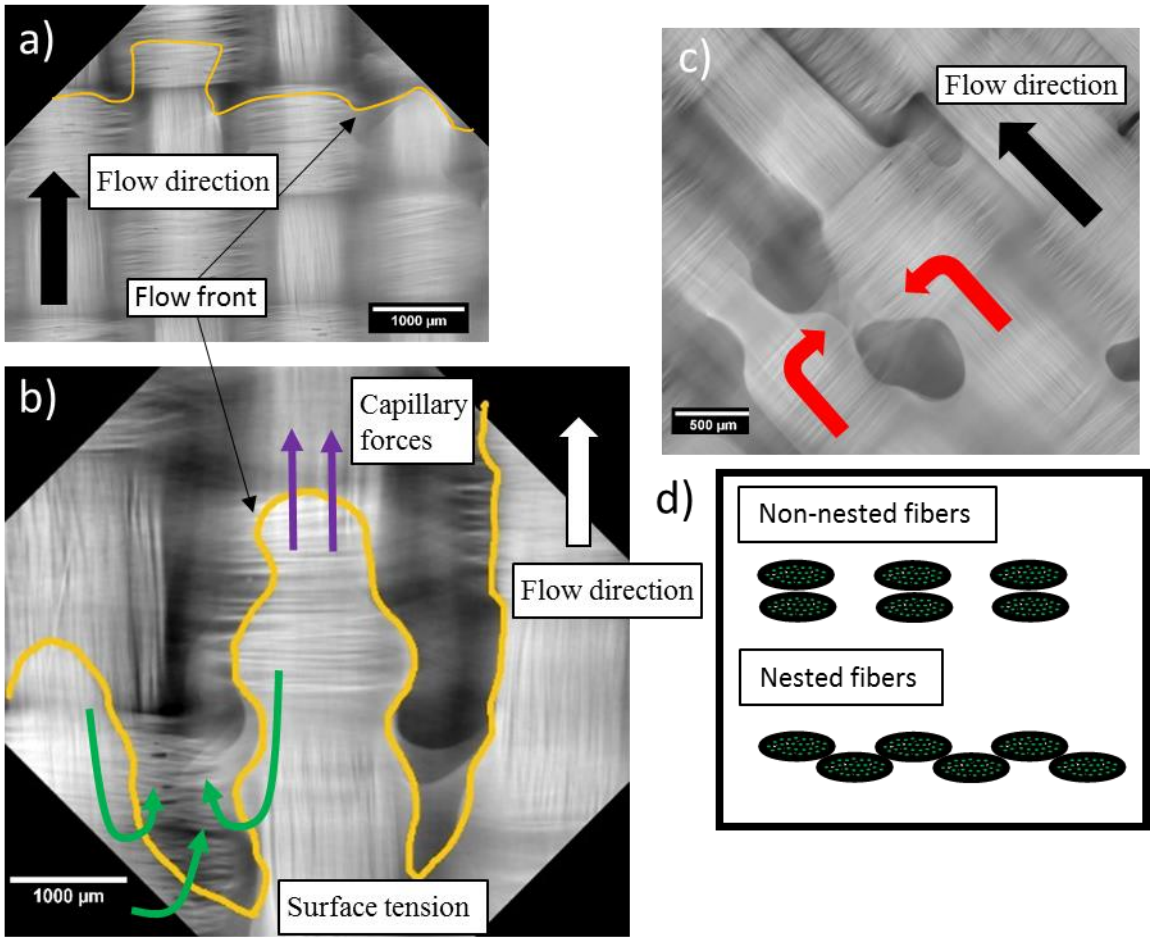

Figure 2. Longitudinal cross section of the impregnated fibers showing the flow front under a) optimal flow conditions (ply 2) and b) low capillary numbers (ply 5). c) shows the moment when two fingerings join together. d) Position of transversal fibers in phase and out of phase.

4. Conclusions

In situ injection experiments were carried out in the synchrotron beam to study the mechanism of flow within a layer of E glass fiber by means of SRCL. A couple of E glass fiber specimens were impregnated with a blend of epoxy resin and a contrast agent using a transparent mold and a peristaltic syringe designed and built for this purpose under constant flow conditions. The high resolution of the SRCL allows the detailed reconstruction of individual tows within the layer while the contrast between the different phases (air, fluid and fibers) was enough to track the fluid front position and shape as well as

the void transport during infiltration. The ability of this technique to analyze the details of microfluid flow and void transport in injection processes is clearly established.

The process of formation and transport of pores has been analyzed by means of SRCL. The void formation has been classified according to the modified capillary number of the process, confirming that the resin flows preferably through the fiber bundles due to the predominance of capillary forces. Additionally, the impact of the geometry on the void formation has been inspected and discussed.

References

[1] N. Patel and L. J. Lee, "Effects of fiber mat architecture on void formation and removal in liquid composite molding," Polym. Compos., vol. 16, no. 5, pp. 386–399, 1995.

[2] N. Patel and L. J. Lee, "Modeling of void formation and removal in liquid composite molding. Part II: Model development and implementation," Polym. Compos., vol. 17, no. 1, pp. 104–114, 1996.

[3] T. S. Lundstrom, "Bubble Transport through Constricted Capillary Tubes with Application to Resin Transfer Molding," Polymer (Guildf). vol. 17, no. 6.

[4] R. Matsuzaki, D. Seto, A. Todoroki, and Y. Mizutani, "In situ void content measurements during resin transfer molding," Adv. Compos. Mater., vol. 22, no. 4, pp. 239–254, 2013.

[5] S. M. Sisodia, S. C. Garcea, A. R. George, D. T. Fullwood, S. M. Spearing, and E. K. Gamstedt, "High-resolution computed tomography in resin infused woven carbon fiber composites with voids," Compos. Sci. Technol., vol. 131, pp. 12–21, 2016.

[6] J. Vilà, F. Sket, F. Wilde, G. Requena, C. González, and J. LLorca, "An in situ investigation of microscopic infusion and void transport during vacuum-assisted infiltration by means of X-ray computed tomography," Compos. Sci. Technol., vol. 119, pp. 12–19, 2015.

[7] N. M. Larson and F. W. Zok, "Insights from in-situ X-ray computed tomography during axial impregnation of unidirectional fiber beds," Compos. Part A Appl. Sci. Manuf., vol. 107, pp. 124–134, 2018.